Time-Dependent One Dimensional Model of MARFES, Detached Plasmas in Divertor Scrape-Off Layer of a Tokamak

R. Goswami, P. K. Kaw, M. Warrier, R. Singh, S. P. Deshpande
Institute for Plasma Research, BHAT, Gandhinagar, Gujarat, INDIA - 382428

Abstract

Analytical and numerical study of the detachment in diverted plasma of a tokamak is presented.The effect of ELMs on detachment has been studied. For high densities and low temperatures near the divertor plate, volume recombination and charge exchange processes seem to play a key role in detachment.

1. INTRODUCTION

The physics of plasma detachment in the divertor region of steady state tokamaks is a topic of current interest. A special area of concern is the investigation of impact of bursts of heat and particles (from a ELMy H-mode core) on the transition from a 'detached' to an 'attached' plasma state in the scrape off layer (SOL). A detached plasma helps to reduce the steady state heat flux as well as the erosion processes on a target plate. This, in turn, reduces the target cooling requirements and increases its lifetime. Recent experiments [1] and simulations [2-3], of the SOL region of a tokamak plasma show that the detachment arises with the drop of plasma temperature, pressure, heat flux and particle flux as one moves along the field lines from the midplane to the divertor plate. In this paper we present some analytic and numerical simulation results of the divertor detachment process based on a time dependent 1-D fluid transport model of the SOL plasma. We first analytically examine the static problem and delineate the conditions for the formation of various fronts associated with radiation, ionization, pressure loss and volume recombination. We then present the 1-D numerical simulation results for a typical detached plasma scenario and ELMs.

2. BASIC EQUATIONS

The 1-D equations are

$$\partial_t n + \partial_x(nv) = S_\perp + n n_n S_i - n^2(S_{rr} + S_{3bd}) \tag{1}$$

$$\partial_t(mnv) + \partial_x(mnv^2) = -\partial_x(nT) - mnv(n_n S_x + nS_{rr} + nS_{3bd}) \tag{2}$$

$$\partial_t[\frac{3}{2}nT + \frac{mnv^2}{2}] + \partial_x[\frac{5}{2}nTv + \frac{mnv^3}{2} - \chi_{||}\partial_x T] = Q_\perp - Q_R - Q_a \tag{3}$$

where all the symbols on the LHS have standard meanings - v and x referring to motion along the field lines, $S_\perp$ and $Q_\perp$ are perpendicular sources of particles and heat into SOL from the core (i.e. from the stagnation point till the null point). The atomic rate coefficients $S_i, S_{rr}, S_{3bd}, S_x$ represent ionization, radiative and 3-body recombination and charge exchange respectively. The energy loss terms are written as $Q_R = n^2\xi_I L(T)$ (radiative loss), Q_a is a sum of thermal and kinetic energy losses due to ionization, recombination and charge exchange. Gains due to 3-body recombination are also retained. The ξ_I is the impurity fraction. Carbon is the only impurity species considered and the impurity density is considered to be a fixed fraction (ξ) of the ion density. A coronal equilibrium model is used in calculating the radiation losses due to carbon impurities [4] which are limited to the region between the divertor plate and the null point. Viscous effects have been neglected. The neutral transport is at present not solved for in the code, although it has been retained in the analysis.

3. ANALYTICAL MODELLING

The physics of thermal fronts has been examined earlier by Hutchinson [5] and the pressure fronts have been approximately dealt with by Ghendrih [6] and Kesner [7] (see [8] for a comprehensive review). The reduced temperatures at the cold side of the thermal front is expected to allow the penetration of the neutrals in the plasma. The density of the neutrals and the local plasma parameters decide the particle, momentum and energy sinks in this region. We consider all these coupled equations for static fronts and present their analytic solutions which

generalises the earlier work by Ewald and Self (see ref [8]) by retaining the energy equation and the equation for neutrals.

The simplified model equations are $d_x(nv) = nn_nS_i - \beta n^3$, $d_xp = -mnn_nS_xv$, $(5/2)d_x(nvT) = -(1/2)mv^2nn_nS_x$, $d_xp_n = -mnn_nS_xv_n$, where n_n is the neutral atoms density and βn is the three-body recombination rate coefficients respectively. The assumptions which go into these equations are: (1) Subsonic flow ($mnv^2 << p$), (2) heat conduction less important than convection ($\chi_{||}T' << nvT$ i.e. $\lambda_{mfp}T'/T << (m_e/m_i)^{1/2}$, valid for low T and high n), (3) division of neutral population in fast and slow neutrals, with momentum and energy loss from the plasma conveyed to the wall by fast neutrals, but neutral population with which plasma interacts consists of slow thermal neutrals, (4) The neutral pressure gradient is neglected in comparison to the plasma pressure gradient, in the calculation of plasma flux (, $= nv$). Here, prime ($'$) indicates differentiation w.r.t x.

Integrating the sum of plasma and the neutrals continuity equations, we get $nv + n_nv_n = 0$ (constant of integration, corresponding to the flux from the hotter side, is taken to be zero). An approximate relation can now be obtained between n_n and n (if we neglect T'/T in comparison to n'/n) as $n_n^2 + \alpha_n n^2 = n_0^2$. The constant $\alpha_n = T(S_x + S_i)/S_xT_n)$. This assumption is only for tractability, and can be relaxed in a detailed analysis.

With $S_x \approx 4 \times 10^{-8} cm^3/s$, one can show that typically the energy loss due to charge exchange is dominant over that due to ionization and recombination. From the energy and momentum equation we obtain, $v = C_1p^{4/5}$ where $C_1 = constant$. Using this in the continuity equation and dividing n' by p' we get,

$$dn/dp = 4n/5p - (S_i - \beta n^2/n_n)p^{8/5}/(mS_x{C_1}^2)$$

We now choose suitable functional forms for T-dependence of S_i and β and assume S_x independent of T. The solution of this equation when substituted in the expression for p' yields p as a function of x.

First, we analyse the solution near the divertor plate (recombination zone) by neglecting S_i. We choose a critical temperature T_r (of the order of 1 eV) below which $\beta \approx \beta_0/T^{18}$ and above which $\beta \approx 0$. In this region, the solution is $n \approx C_rp^{77/95}$, which shows that density decreases as the pressure drops towards the plate. Above the critical temperature, i.e., when $p/n = p^{18/95}/C_r > T_r$ one obtains the 'constant-flux' solution, $n = C_mp^{4/5}$. The behaviour of p is approximately given by $p(x) = \text{const.} \times x$.

We now discuss the solution in the ionization zone. In this region we drop the recombination term and model S_i as S_0T^6 (so that $10^{-13} \leq S_x \leq 10^{-9} cm^3/s$ in the range $1 \leq T_eV \leq 4$). The relevant equation is $\frac{dn}{dp} = \frac{4n}{5p} - \alpha_i p^{38/5}/n^6$, which can be integrated to yield $n = p^{4/5}(C_i - (7/3)\alpha_i p^3)^{1/7}$, where C_i is a constant of integration, and $\alpha_i = S_0/(C_1^2 mS_x)$. When p is small (towards the plate) we get the constant flux solution, with $C_i^{1/7} = C_m$. We must mention here that $p(x)$ in the ionization zone is obtained initially as $x = x(p) \sim$ Const. $\times$ F(1/3,1/7;4/3;p^3) (hypergeometric series). As one approaches the hot zone, the flux ($\propto np^{-4/5}$) drops, as expected by the observation that the ionization source should have increased , ($= nv$) from the midplane value (assumed to be small). Furthermore, as the neutral population is expected to drop towards the hotter side, the charge exchange friction is unable to support the pressure gradient. This zone, where there are no sources of particles and energy needs some careful treatment as it connects the conduction dominated region (just after the thermal front) and the ionization dominated region. The relevant equations are $nv =$, $=$ Const., $\frac{d}{dx}(p + mnv^2) = 0$, $\frac{d}{dx}(5nvT/2 - \chi_{||}\frac{dT}{dx}) = 0$. From these we get $\frac{5p\Gamma}{2n} - \frac{2}{7}\frac{d}{dx}(p/n)^{7/2} = W$, the heat flux coming out of the thermal front. This equation can be easily integerated exactly to yield $T(x)$ from which n, p and v can be obtained. The assumption of small v allows one to match the solutions in this and the ionization zone.

4. NUMERICAL RESULTS FOR DETACHMENT AND ELMS

A time dependent 1-D code which solves the plasma fluid transport equations [9] along the field lines, using a flux corrected transport algorithm [10] has been developed. The neutral profile is specified as $n_n(x) = n_n(x_d)e^{-\int \frac{dx}{\lambda(x)}} + n_{bg}$, where $n_n(x_d)$ is the neutral density at the divertor plate and $\lambda(x)$ is the neutral penetration length which depends on x through the local plasma density n and temperature T, and n_{bg} is the background neutral density. A connection length of 30 m (x_d) with the null point at 21 m (x_x) was assumed. The boundary conditions imposed are $n'(0) = T'(0) = v(0) = 0$ and v at $x_d = C_s$ (local sound speed). Heat flux at x_d equated to local $\gamma n C_s T$, where γ is the sheath energy transmission factor. We also impose a flexible boundary condition that $n''(x_d) = 0$ [11].

A converged result for a detached case with $S_\perp = 8 \times 10^{22} m^{-3} s^{-1}$, $Q_\perp = 6 MW/m^3$ and $n_{bg} = 5 \times 10^{16} m^{-3}$ is shown in Fig.1. In Fig.1 the mid-plane is at 0 and the divertor plate sheath edge is at the other end. Fig.1a shows a sharp drop in plasma temperature at $\sim$ 26 m, corresponding to a peaked impurity radiation (Fig.1b) and a sink of ionization energy loss (Fig.1c). The fluid velocity also reaches supersonic speeds before this region and suddenly plummets to a very low, more or less constant value after this point(Fig.1e). The plasma density jumps up at this point (Fig.1d). The ionization sources due to n_{bg} dominates $S_\perp$ in the region between the mid-plane to null point.

The above observations are a result of the neutrals, which under conditions favourable for detachment attain a profile shown in Fig.1f, similar to a gas box in front of the divertor plate. Such a profile for neutrals is got because $\lambda(x)$ becomes very large at T $\sim$ 1 - 2 eV. Therefore the neutral profile is almost flat. This continues till higher values of T are encountered and $\lambda(x)$ becomes small. Then the neutral density drops rapidly. The plasma flowing at supersonic speeds suddenly encounters this high density gas target and the large momentum sink due to charge exchange causes it to fall and attain a constant value. The density rise is mainly due to the fall of velocity and to a lesser extent due to ionization sources at the front position. The increased plasma density causes the impurity density (which is pegged at ξ_I times the plasma density) to increase and therefore gives an increased impurity radiation, which is a major sink in the energy equation (Eqn.3). This causes a thermal front at the location where the velocity falls (i.e. where the gas box begins). This is also the location where there is a peak in ionization. Beyond this point the temperature is too low to cause ionization. The plasma density falls in the low temperature region due to recombination. This is what causes a fall in the particle flux.

Parameter scans were carried out keeping $Q_\perp$ constant at 4 MW/m^3 and $S_\perp$ taking values $4-6 \times 10^{22}/m^3/s$. We do not get detachment for these reduced values of $S_\perp$, though $S_\perp = 6 \times 10^{22}$ results in low temperatures at the divertor plate $\sim$ 4 eV, at which volume recombination is not large. Then in the second set of runs keeping $S_\perp$ constant at $8 \times 10^{22}/m^3/s$ we take $Q_\perp$ values of 4 to 6 MW/m^3. These runs also show that for higher values of $Q_\perp$ detachment is lost. When n_{bg} is reduced to $5 \times 10^{15} m^{-3}$, $Q_\perp = 2 MW/m^3$ and $S_\perp = 6 \times 10^{22} m^{-3} s^{-1}$ we get detached solutions with subsonic flows.

Two types of ELMs, type I giant ELMs and type III grassy ELMs were modelled. For the giant ELMs and grassy ELMs the ELM time was taken to be 1 millisecond and 0.1 millisecond respectively and the dwell time between ELMs was taken as 8 milliseconds and 0.7 milliseconds respectively. Three cases were considered for the giant ELMS depending on the enhancement in $S_\perp$ and $Q_\perp$. $S_\perp$ and $Q_\perp$ were enhanced by 20 % and 20 %, by 20% and 10 % and by 10 % and 20 % respectively. For the grassy ELMs only the case with 5 % enhancement in $S_\perp$ and $Q_\perp$ was considered.

In all the cases for giant ELMs we see that the detachment front does not shift during the ELM but after the ELM subsides, it moves towards the null point. The distance shifted increases as the enhancement to $S_\perp$ is increased and is marginal for changes in $Q_\perp$. In the case of grassy

ELMs the detachment front position is not affected at all. In all cases we see increased impurity radiation and increased ionization during ELMs at the front location.

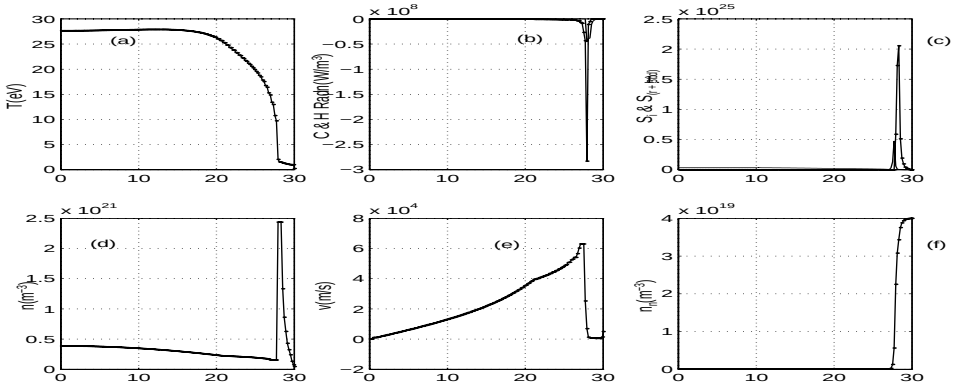

Figure 1: Plasma parameters as a function of the connection length

5. CONCLUSION

In conclusion, we have presented analytic and numerical results of a 1-D model of plasma detachment. The main result of the analytic work is the derivation of closed form solutions connecting the cold edge of thermal front to the divertor plate by a multi-region analysis involving ionization, momentum loss and volume recombination effects. Our numerical simulations gave an example of a convection dominated detachment front in which ionization and radiative phenomena are essentially superposed at the same location. Similarly, our ELM simulations were optimistic showing that even giant ELMs don't lead to attachment in this parameter space. It is conceivable that some of our numerical results can get significantly modified if we retain some of the neglected effects such as (i) parallel viscous drag on the flow, (ii) a density feedback fixing the midplane density of the plasma, (iii) 2-D effects increasing the flaring of the SOL, etc.

REFERENCES

1. T. Petrie et al., J. Nucl. Mater., 196-198 (1992) 849.
2. K. Borass, D. P. Coster and R. Schneider., "24^{th} EPS Conference on Controlled Fusion and Plasma Physics," Berchtesgaden, 9^{th} – 13^{th} June 1997, Pg.1461
3. Gary D. Porter, et al., *Phys. Plasmas* 3 (5) (1996) 1967.
4. D. E. Post and R. V. Jensen, *Atomic data and nuclear data tables*, 20 (1997) 397.
5. I. H. Hutchinson, *Nucl. Fusion* 34 (1994) 1337.
6. Ph. Ghendrih, *Phys. Plasmas* 1 (6) (1994) 1928.
7. J. Kesner, *Phys. Plasmas* 2 (6), (1995) 1982.
8. C. S. Pitcher and P. C. Stangeby, *Plasma Phys. Control. Fusion* 39 (1997) 779-930.
9. S. I. Braginskii, *Reviews of Plasma Physics* Vol.1 (1965) 205.
10. Jay P. Boris and David L. Book, " LCPFCT code" *NRL Report 1994.*
11. J. Neuhauser, et. al., *Nuclear Fusion* , Vol.24, No.1 (1984) 39.